AIR BUBBLES INFLUENCE ON WAVE BREAKING: AN EXPERIMENTAL STUDY

Djalal Merkoune[1], Nizar Abcha[1], Dominique Mouazé[1], Alexander.Ezersky[1]

Abstract

We report experimental results on influence of air bubbles curtain on wave breaking realized in experimental wave flume with water depth of 45 cm. It was found that position of wave breaking point depends on bubble density in water. It was revealed that the effect of wave breaking is very sensitive to the concentration of air bubbles near free surface of water. We showed that a small concentration of artificially created bubbles do not lead to additional dissipation of energy in surface waves but change sufficiently the position of wave breaking point. To understand physical mechanisms of bubbles - wave breaking interaction, we studied the velocity of bubbles using double-tip conductivity probes which is based on the electrical resistance, and vorticity fields of flow caused by rising bubbles using Acoustic Doppler Velocimetry (ADV).

Key words: Breaking waves, air bubbles**,** hydrodynamic, velocity, dissipation of energy, surface waves.

1. Introduction

Breaking of water waves plays an important role in many processes in coastal dynamics. This phenomenon is accompanied by the appearance of turbulent zones and clouds of air bubbles. Many studies have been made on characteristics of turbulence and bubbles generated by breaking wave. For example size distributions of bubbles have been studied in details for natural conditions Grant, B. and Deane, M. (1998) and in numerical simulations Mukherjee A and Kandlikar, S. G (2006). It should be noted that the process of wave calming by injecting of air bubbles beneath the water surface has been discussed for century Cummings, P.D and Chanson H (1997). It was found that intense curtain of air bubbles can sufficiently reduce the amplitude of surface wave. In nature, air-water flows are observed not only in breaking waves in coastl zone, but also in waterfalls, in mount rivers characterized by a steep slope and in wave breaking. This mixture is also observed in the hydraulic structures Chanson, H. and Lee, J.F. (1997). The first experimental studies Wood, I.R. (1991), Hager, W.H. and Kramer, K. (2003) have been made since decades to show the complexity of the aeration process of the free surface. Different parameters have been subjected to analysis. We mention in particular the density of the mixture John D. Ditmars and Klas Cederwall (1970), the dispersion of bubbles in a mixture Hinata et al (1977) and the mean flow velocity Wood I.R., (1984), Kobus, H. E. (1968).To understand the process of air training in flowing water, numerical modeling and analytical the solutions have been attempted by many researchers. The results of these studies highlight the major role of this phenomenon in the process of energy dissipation due to strong turbulence generation Lubin et al (2006), Guignard et al (2001). The main problems are the analysis of the steps emergence and evolution of air pockets in the water flow. Vassilev A et al (2007) determined experimentally and numerically the flow characteristics and the 2D shape of gas bubble immersed in a liquid or stagnation flow. This study examined the spatiotemporal evolution of air – water mixture in the case where the viscosity influences on movement of the bubbles.

In the presented paper we concentrate our attention on the following problem: how a small amount of artificially generated air bubbles influences the wave breaking. We performed detailed analysis of position of wave breaking point and characteristics of hydrodynamic flow in the vicinity of air bubble curtain.

The paper is organized as follows: the experimental system and procedure are described in section 2. The results are presented in section 3, section 4 contains conclusion.

[1] Laboratoire de Morphodynamique Continentale et Côtière UMR 6143 CNRS. djalal.merkoune@gmail.com

2. Experimental set-up

Experiments were carried out in a wave flume with a length of L=22 m, a width of D=0.8 m and a water depth of H=0.5 m. At one end of the channel wave-maker was situated, at the other end a porous beach (PB) was installed to minimize wave reflection (Figure 1). We used computer controlled wave-maker to generate periodically propagating wave trains with frequency modulation. Initial duration of wave train was approximately 12 seconds and period of repetition was close to 30 seconds. The modulation frequency of wave train results in dispersion focusing of surface waves: decreasing of impulse duration and increasing of its amplitude along the channel. Such a process called dispersion focusing, led to the wave breaking at a definite distance from the wave-maker. Position of wave breaking was defined by the amplitude of wave train and index of frequency modulation. In our experiments the length of focusing was approximately 14.5 m.

We studied the influence of artificially created bubbles on dynamics of surface waves. The bubble curtain was generated at a certain distance from the wave maker where amplitude of wave train did not reach yet critical value corresponding to wave breaking. To create the curtain we placed on the bottom of channel cylindrical tube connected with an air pump. Axis of tube was perpendicular to the lateral wall. Small holes of the same diameter were drilled periodically in the wall of the tube to generate air bubbles. We investigated the evolution of free surface displacement of nonlinear wave for different values of air flux and, consequently, for different concentrations of air bubbles in curtain.

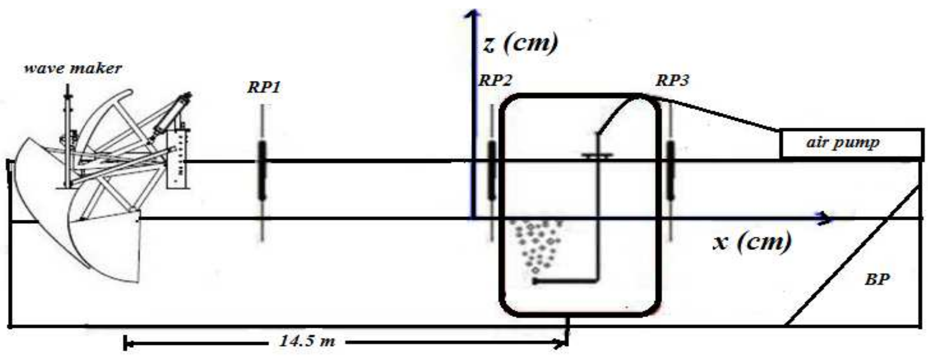

Figure 1**.** Experimental setup: RP1, RP2, RP3 are resistive probes free surface measurement, PB is porous beach.

The air-water flow properties were measured with a double-tip conductivity probe (Figure 2a). The conductivity probe is a phase-detection intrusive probe designed to pierce the bubbles. Its operation is based on the difference in electrical resistance between air and water Crowe et al. (1998), Chanson (2002). The dual-tip probe was equipped with two identical sensors. The distance between probe tips was $\Delta x = 3$ mm (Figure 2a). Sensors of dual-tip probe were connected with Wheatstone bridges measuring electrical resistance. Negative impulses in Figure 2b correspond to air bubbles passing through the first probe (curve 1) and second probe (curve 2). Signal from each probe was sampled at 5 kHz for during 10 s. Vertical position of the dual-tip probe was controlled by a system of displacement with precise accuracy of 1 mm (Figure 2b).

To measure velocity of bubbles, cross correlation function of two signals were calculated (Figure 2c). This velocity V was estimated as $V = \Delta X/\Delta T$ where Δx is the longitudinal distance between both tips ($\Delta x = 3$ mm) and ΔT is the time delay of the signal from the second probe Crowe et al. (1998), Chanson (2002).

Air bubbles rising from the bottom induced large scale motion in the flume. To investigate the characteristics of this flow, the Acoustic Doppler Velocimetry (ADV) Nortek™ Vectrino was used. This ADV with high working frequency of ultra sound (10MHz) allowed us to measure two instantaneous velocity components at a single-point. To perform the measurements of velocity field it was necessary to add into water micro particles providing scattered ultrasound. Due to high working frequency, the spatial resolution of ADV is 6 cm.

The free surface profile was recorded by means of a high-speed camera. The image analysis is processed frame by frame to gives of the qualitative information on characteristics of free surface near point of wave breaking. The horizontal coordinate corresponding to the vertical tangent of free surface of water was considered as a point of wave breaking.

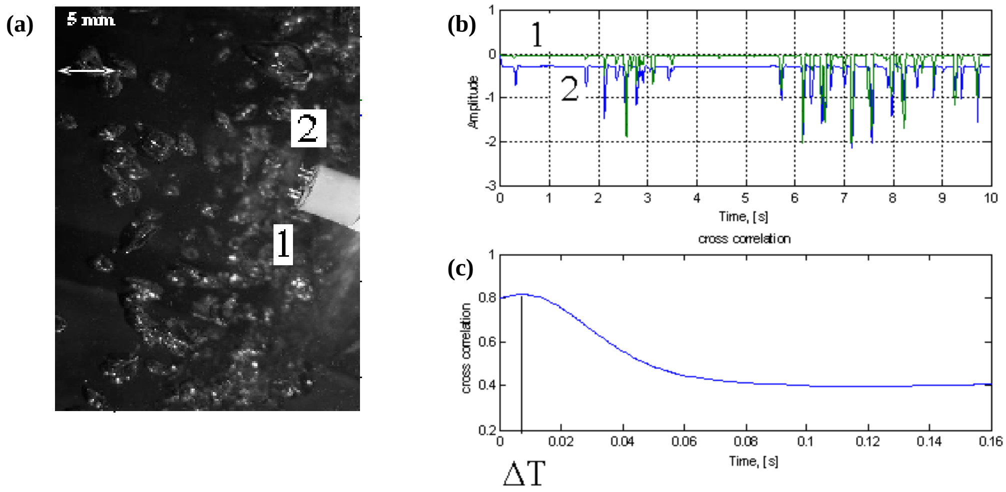

Figure 2: a) photograph of the double-tip conductivity probe. b) double-tip conductivity probe outputs. c) cross-correlation function for a dual-tip probe

3. Results

3.1. Behavior of breaking waves in the presence of air bubble curtain

To study the influence of air bubbles on process of wave breaking, we conducted two types of experiments. In the first type of experiments bubbles were generated by aeration pump continuously. In this case we revealed that position of the of wave breaking point essentially depends on air flux, and even small concentration of artificially generated bubbles led to the displacement of wave breaking point in the direction to the wave maker. A change in position of wave breaking point is shown in Figure 3. The most large influence of bubbles is observed for air flux increasing from zero to $0.2.10^{-3}$ m^3/s. Displacement of the wave breaking point $(X\text{-}X_0)$ towards the wave maker attains 50cm, where X_0 =13m corresponds to the position of wave breaking point for zero air flux $Q=0$.

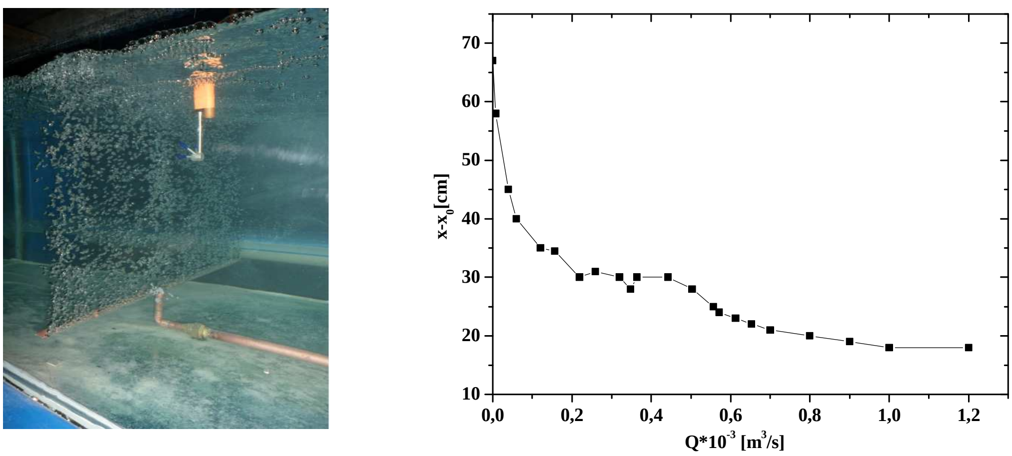

Figure 3 a) photograph of air bubbles curtain. b) Dependence of wave breaking coordinate $(X\text{-}X_0)$ on flux Q

In the second type of experiments we investigated wave breaking after stopping artificial water aeration. Experiments were organized as follows: generation of bubbles occurred during several minutes by an air flux Q = 1.2 10^{-3} m^3/s., thereafter air pump was stopped. During several minutes, air bubbles were rising to the water surface and influence of water aeration on wave breaking was observed in experiment. The dependence of the displacement of the wave breaking point on time after stopping the aeration is shown in Figure 4. We conducted six tests to see the reproducibility of results obtained. It should be noted that in our experimental condition the aeration retains its influence during approximately 5 minutes.

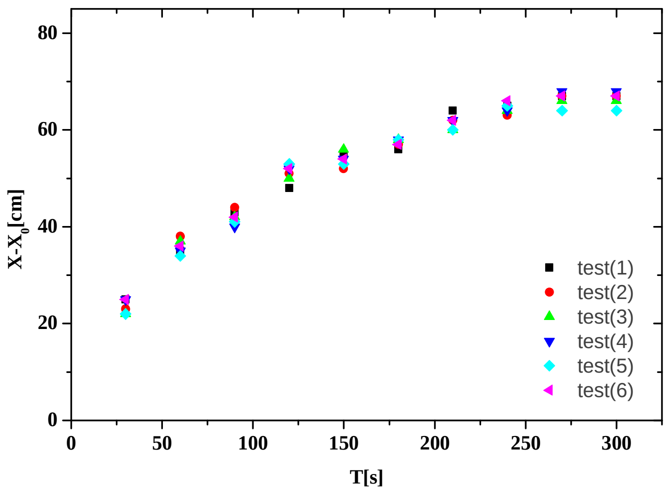

Figure 4. Dependence of wave breaking coordinates on time. At t=0 air compressor was stopped.

3.2. **Wave energy in the presence of a bubble curtain**

To investigate the influence of bubbles on wave breaking more precisely we studied the changes of energy of wave train for different air-flux. We show in Figure 5 the evolution of a wave packet in the flume. This evolution is analyzed in the presence of a bubble curtain in order to examine the impact of the presence of bubbles on the energy of the wave. The wave packet energy (energy on a unit length in the direction transversal in the direction of wave propagation) is estimated as follows:

$$E = \frac{gD}{2}\int v_g(\omega)\left|S(\omega)\right|^2 d\omega \qquad (1)$$

g is acceleration of gravity, $\boldsymbol{v_g}$ is group velocity, S(w) is Fourier spectrum of surface wave elevation h.

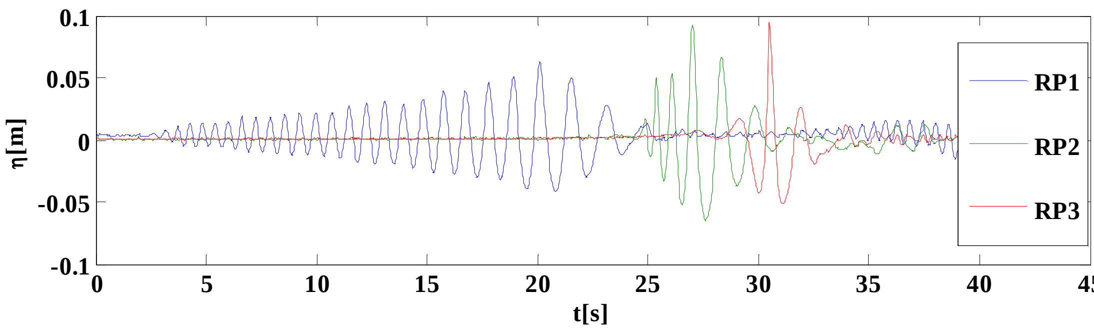

Figure 5. Evolution of wave packet along the channel. Time series of free surface displacement η are recorded by three transducers for a pulse with averaged frequency f=0.75 Hz.

Our calculations showed us that this integral practically coincides with the following expression:

$$E = \frac{gD}{2} v_g \int_0^T \eta^2 dt \tag{2}$$

v_g is group velocity of spectral maximum, T is duration of wave train. We examined energy of time series obtained by resistive probes RP1, RP2, RP3 in different points along the channel as a function air flux Q. Results are presented in Figure 6. Bubble curtain does not influence on wave train energy before the wave breaking point, there exist small decreasing of the energy due to viscous dissipation (curves RP1 and RP2, Fig. 6). Wave train energy after wave breaking point slightly depends on air flux Q (curve RP3). Our experiments have shown that the supplementary energy dissipation introduced by artificially created air bubbles is very low in comparison with energy dissipation due to wave breaking.

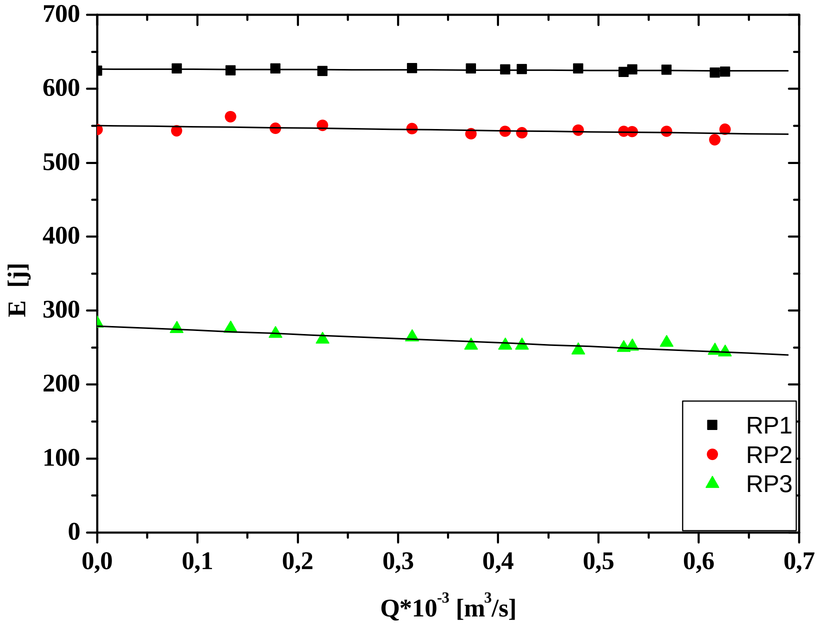

Figure 6. Dependence of wave packet energy on air flux; probes PR1,2 are situated in the flume before wave breaking point, PB3 is behind this point. .

3.3. Velocity profiles of bubbles

In the absence of waves, the width of air bubbles curtain increases symmetrically towards to free surface. Using a double-tip conductivity probe we have measured the vertical velocity of bubbles versus the water depth (Figure 7).

Near the flume bottom, air bubbles have high velocities few tens of centimeters/second. One can distinguish two zones of bubble curtain. In the first one velocity of bubbles increased, and at height of 24 cm reached a maximum value of 0.48 m/s. In the second zone, beyond height (z >24 cm) velocities decreased to zero at the free surface. This decrease is due to interaction of the bubbles with large scale motion generated near the curtain.

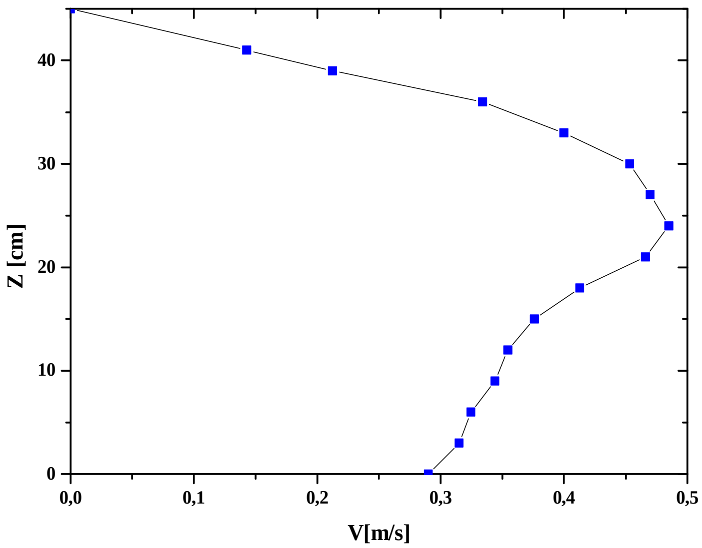

Figure7. Vertical velocity of bubbles versus vertical coordinate z for an air flux Q = 1.2 10^{-3} m^3/s.

The longitudinal profile of the vertical velocity at a position close to it maximum (z = 22cm) and at z = 37cm are shown in Figure 8. Coordinate x = 5 corresponds to the position of the axis of the bubble curtain. The width of the curtain was about 6cm, thus there were no data for large distance from the center line curtain. It should be noted that maximal velocity of bubbles is approximately 45 cm/s. It should be noted that the same value of bubble velocity we obtained using movie filmed by high speed camera. It is known that velocity of single air bubble rising in water grows with diameter. If its diameter is less than 1 cm, velocity is complex function of Reynolds number, it depends on bubble shape and initial condition see Kulkarni et al (2005). For diameter of bubble more 1cm velocity V may be estimated as $V \approx \sqrt{gd/2}$. For our experiments diameter of bubble d is less that 1 cm, that is why its velocity should be less than $V \leq 22 cm/s$. In fact velocity is two times more. It means that in the curtain, chain of rising bubbles generates additional vertical component of velocity.

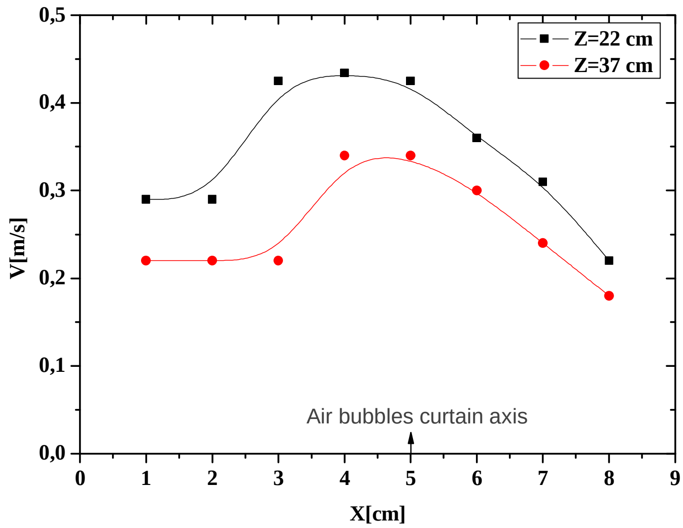

Figure 8. Horizontal profile of vertical velocity of bubbles for two depths (air flux Q = 1.2 10^{-3} m^3/s).

3.4. Velocity field of flow generated by bubbles

Double-tip conductivity probe allowed us to measure bubble velocity. Rising bubbles set in motion water at all depths in the vicinity of the curtain. It creates large scale motion in the flume. In order to understand the structure of large scale velocity field, Acoustic Doppler Velocimeter was used. Two component of velocity were measured in the absence of waves, for the same air-flow bubbles conditions as for the test carried for velocities measurement of bubbles ($Q = 0.4\ 10^{-3}$ m3/s and $Q = 1.2\ 10^{-3}$ m3/s).

Acoustic Doppler Velocimetry (ADV) measurements have been made in 414 points. Vertical velocity profiles have been carried out along 1.34 m (67 cm on each side of the curtain of bubbles).

At each measurement point, data acquisition was performed during 30s with an acquisition frequency of 200 Hz. Figure 9a shows the distribution of time-averaged velocity fields.

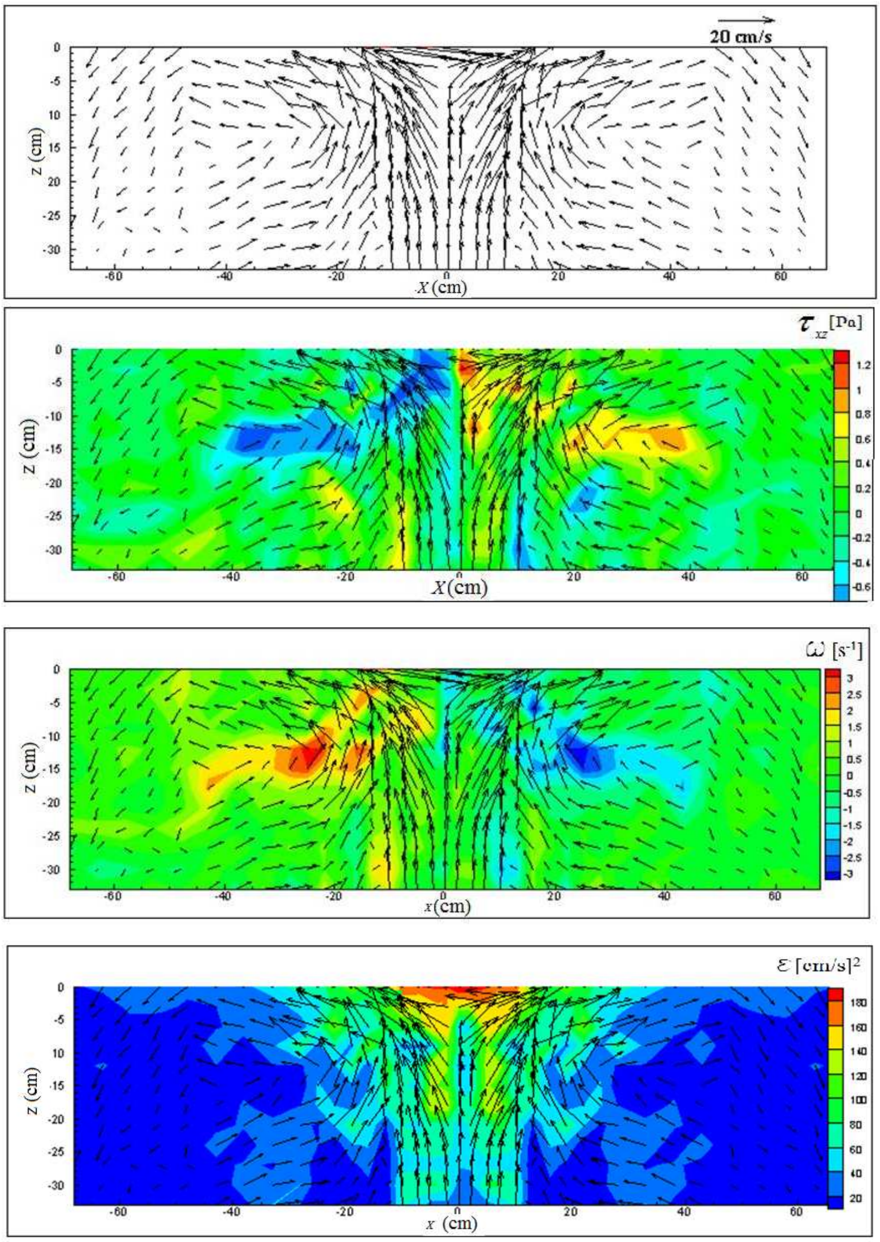

Figure 9. Fields generated by air bubble curtain, air flux $Q = 1.2\ 10^{-3}\ m^3/s$: a) velocity fields, b) vorticity fields, c) shear rate fields, d) kinetic energy fields.

We observe that the flow generated by air bubbles is vertically ascending in the vicinity of the bubble curtain. This ascending flow becomes horizontal near the free surface. From both sides of the curtain, two large circulating cells take place in the flume: an anti-clockwise circulating cell at the left of curtain and a clockwise circulating cell at the right.

Time-averaged velocity fields (v_x, v_z), allowed us to determine quantities characterizing the large scale flow:

- the vorticity: $$\omega = \left(\frac{\partial v_x}{\partial z} - \frac{\partial v_z}{\partial x} \right)$$
- the shear rate: $$\tau_{xz} = \mu \left(\frac{\partial v_x}{\partial z} + \frac{\partial v_z}{\partial x} \right),$$ μ is dynamical viscosity of water
- the density of kinetic energy: $$\varepsilon = \frac{v_x^2 + v_z^2}{2}$$

Figure 9 shows the velocity field (Fig. 9a), and component of vorticity field (Fig. 9b), shear rate (Fig.9c), kinetic energy density (Fig.9d) on the background of the velocity field. It is possible to note that maxima of

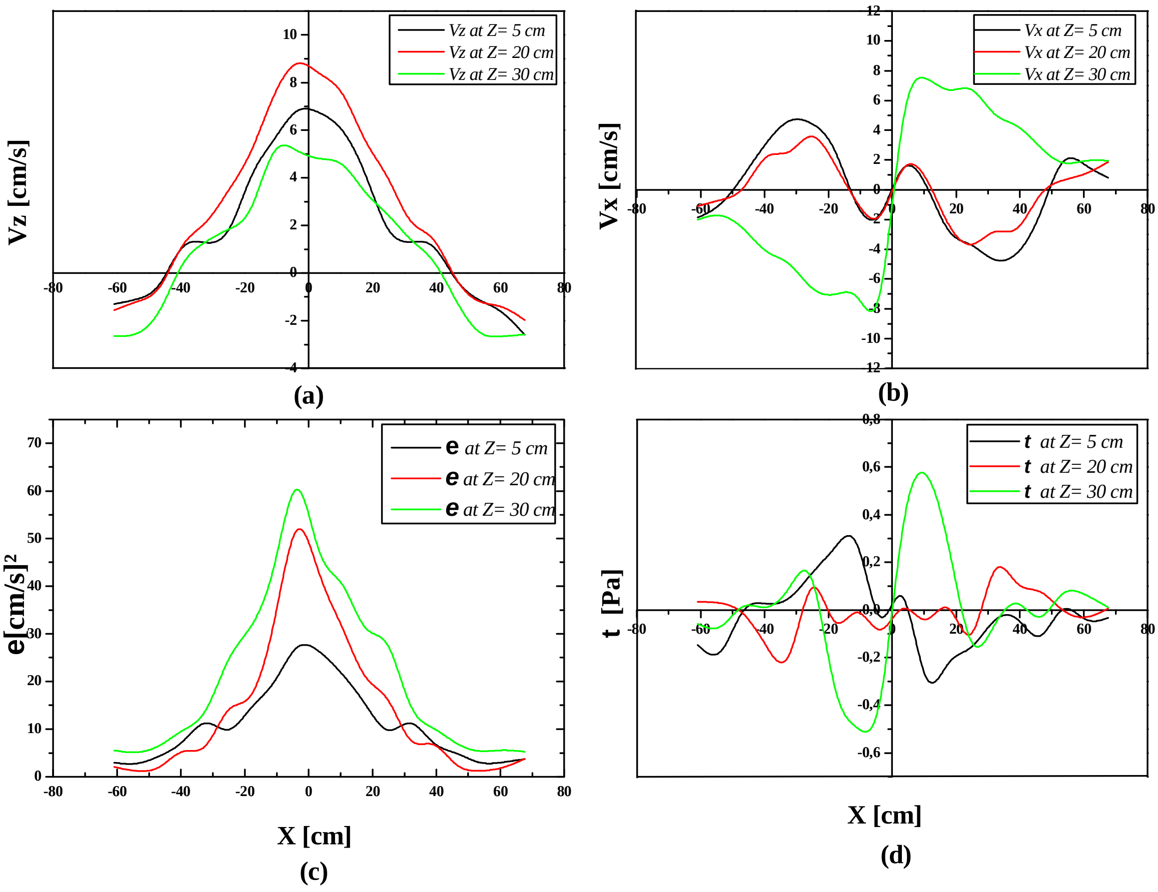

Figure10. The horizontal profiles at three positions (Z = 5cm, Z = 20cm and Z = 35cm from the bottom) : a) the vertical velocity $V_z(x)$; b) horizontal velocity $V_x(x)$; c) kinetic energy $e(x)$; d) the shear rate $\tau_{xz}(x)$

vorticity field are situated at the centers of two counter rotating vortices approximately at half of water depth (Fig.9b). The maximum of kinetic energy density occurs in a layer just below the free surface in the center of bubble curtain. Figure 9d shows that domain of high kinetic energy density is observed where the flow changes its direction from the vertical to the horizontal one. The shear rate $\tau_{xz}(x)$ field has maxima near the free surface and in the centers of vortices.

From this time-averaged velocity fields, we have extracted the horizontal profiles of different quantities characterizing the flow at three positions versus water depth (z = 5cm, z = 20cm and z = 35cm from the bottom). Figure 10 shows the vertical and horizontal velocity $V_x(x)$, $V_z(x)$, the shear rate profile $\tau_{xz}(x)$ and kinetic energy profile $\varepsilon(x)$. All profiles show symmetry relatively to the axis of the curtain of bubbles. The vertical velocity $V_z(x)$ reaches its maximum at mid-depth of the water column while the horizontal velocity $V_x(x)$ reaches its maximum near the bottom and near the free surface at the inlet and at the outlet of the flow cell. It should be noted that velocity of water in the vicinity of curtain is less than velocity of rising bubbles, generated large scale vortices.

4. Conclusion

We have demonstrated experimentally that artificially created air bubble curtain can accelerate wave breaking. According to our results such effect is observed for air bubbles concentration which introduces very small energy dissipation in comparison with energy dissipation due to wave breaking. In our opinion this phenomenon could be very important to coastal dynamics. Suppose, for example, that after the breaking of the first wave a cloud of air bubbles appears. Air bubbles could accelerate the breaking of the next wave and lead to the further increasing of bubble concentration. It influences the breaking of the next waves and etc. Finally local zones with high concentration of bubbles could appear in the upper layer of the ocean.

The physical mechanisms leading to the acceleration of the wave breaking may be related to two effects. Our measurements show that the rising bubbles lead to the appearance of high shear stresses near the free surface. These shear stresses can significantly affect the wave breaking. At the free surface, the rising bubbles reduce the density of the water-air mixture. Decrease in density near the free surface can also accelerate the wave breaking. The question which of the two physical effects dominates requires further study.

References

Vassilev A, Ben Hadid H, El Hajem M, Botton V "Experimental and numerical investigation of an air pocket immersed and immobilized in a horizontal water duct flow" *International Journal of Heat and Fluid Flow* 28 (2007) 673–682.

Chanson, H., and Manasseh, R. 2003. "Air Entrainment Processes in a Circular Plunging Jet. Void Fraction and Acoustic Measurements". *Journal of Fluids Engineering*, Trans. ASME, Vol. 125, No. 5, Sept., pp. 910-921.

Chanson, H. and LEE, J.F. 1997. "Plunging jet characteristics of plunging breakers". *Coastal Engineering*, 31(1–4), 125–141.

Chanson, H. and Carosi, G. 2007. "Advanced Post-Processing and Correlation Analyses in High-Velocity Air-Water Flows". *Environmental Fluid Mechanics*, Vol. 7, No. 6, pp. 495-508.

Cummings, P.D and Chanson H. 1997. "air entrainment in the developing flow region of plunging jets-Part1: theoretical de development ". *J. Fluids Eng.* 119(3), 597-602.

John D. Ditmars and Klas Cederwall 1970 "analysis of air-bubble plumes"coastal engineering v 128 PP 2209-2226.

Hager, W.H. and Kramer, K. 2003. "Historical Development of Free-Surface Chute Aeration". *Proc. 30th IAHR Biennial Congress, Thessaloniki, Greece, J. GANOULIS and P. PRINOS Ed.*, Vol. E, pp. 389–396.

Hinata, S., Kuga, O. and Kobayasi, K. 1977. "Diffusion of bubbles in two-phase flow. I - On the method for the measurement of the diffusivity of the bubble". *JSME*, vol. 20, p. 1299-1305.

Grant, B. Deane, M. Dale Stokes., 1998. "Air Entrainment Processes and Bubble Size Distributions in the Surf Zone" *Journal of Physical Oceanography* 29, 1393–1403.

Guignard, S., Marcer, R., Rey, V., Kharif, C. and Fraunié, P., 2001. "Solitary wave breaking on sloping beaches: 2-d two phase flow numerical simulation by slvof method". *Eur. J. Mech. B, Fluids* 20, 57–74.

Kucukali, S. and Chanson, H. 2008. "Turbulence Measurements in Hydraulic Jumps with Partially-Developed Inflow Conditions". *Experimental Thermal and Fluid Science*, Vol. 33, No. 1, pp. 41-53.

Kobus, H. E. 1968. "Analysis of the Flow Induced by Air-Bubble Systems". *Coastal Eng. Conf., London*, Vol. II, p. 1016.

Mukherjee, A. Kandlikar, S. G.. 2007. "Numerical study of single bubbles with dynamic contact angle during nucleate

pool boiling ". *International Journal of Heat and Mass Transfer* 50 (2007) 127–138.
Murzyn, F. and Chanson, H. 2009. "Two-Phase Gas-Liquid Flow Properties in the Hydraulic Jump: Review and Perspectives, Multiphase Flow Research". *Nova Science Publishers*, Hauppauge NY, USA, Ed Martin. S and Williams J.R., Chapter 9, pp. 497-542 (ISBN 978-1-60692-448-8).
Lubin, P., Vincent, S., Stéphane, A. and Caltagirone, J.P 2006. "Three-dimensional Large Eddy Simulation of air entrainment under plunging breaking waves " *Coastal Engineering* 53 631–655.
Vassilev, A. Ben Hadid. H., Ben El Hajem. M. and Botton V. 2007. "Experimental and numerical investigation of an air pocket immersed and immobilized in a horizontal water duct flow". *International Journal of Heat and Fluid Flow* 28 673–682.
Wood, I.R., 1984. "Air Entrainment in High Speed Flows". Proc. Intl. Symp. on Scale Effects in Modelling Hydraulic Structures, *IAHR, Esslingen*, Germany.
Wood, I.R.. 1991. "Air Entrainment in Free-Surface Flows". *IAHR Hydraulic Structures Design Manual* No. 4, Hydraulic Design Considerations, Balkema Publ., Rotterdam, The Netherlands, 149 pages.
Kulkarni, A.A. and Joshi J.B. 2005. "Bubble formation and bubble rise. Velocity in gas-liquid sustems; A rewiew". *Ind. Eng. Chem. Res.* 44, 5873-5931.